Overcharging of a macroion by an oppositely charged polyelectrolyte

T. T. Nguyen, B. I. Shklovskii

Department of Physics, University of Minnesota, 116 Church St. Southeast, Minneapolis, MN 55455, USA

Abstract

Complexation of a polyelectrolyte with an oppositely charged spherical macroion is studied for both salt free and salty solutions. When a polyelectrolyte winds around the macroion, its turns repel each other and form an almost equidistant solenoid. It is shown that this repulsive correlations of turns lead to the charge inversion: more polyelectrolyte winds around the macroion than it is necessary to neutralize it. The charge inversion becomes stronger with increasing concentration of salt and can exceed 100%. Monte-Carlo simulation results agree with our analytical theory.

PACS: 87.14.Gg, 87.15.Nn

Keywords: Charge inversion, polyelectrolyte, spherical macroion

I. INTRODUCTION

Electrostatic interactions play an important role in aqueous solutions of biological and synthetic polyelectrolytes (PE). They result in the aggregation and complexation of oppositely charged macroions in solutions. For example, in the chromatin, negative DNA winds around a positive histone octamer to form a complex known as the nucleosome. The nucleosome was found to have negative net charge Q^* whose absolute value is as large as 15% of the bare positive charge of the protein, Q. This counterintuitive phenomenon is called the charge inversion and can be characterized by the charge inversion ratio, $|Q^*|/Q$. For PE-micelle systems, charge inversion has been predicted by Monte-Carlo simulations [1] and observed experimentally [2].

These and other examples have recently stimulated several theoretical studies of charge inversion accompanying the complexation of a flexible PE with a rigid spherical or cylindrical macroion of opposite sign [3–6] (for more extensive bibliography on this subject see Ref. [4]). All these authors arrive at the charge inversion for such a complexation. It was also shown that if the PE molecule is not totally adsorbed at the surface, its remaining part is repelled by the inverted charge of the macroion and forms an almost straight radial tail [3,4](see Fig. 1). However, all these papers use different models and seemingly deal with charge inversion of different nature. Surprisingly, both Refs. [3,4] show that the inverted charge of a macroion Q^* does not depend on the value of the bare charge Q.

In this paper we present a new theory of complexation of a flexible PE with an oppositely charged rigid sphere. We consider here only the case of a weakly charged PE which does not create Onsager-Manning condensation. We show that both in salt free and salty solutions the charge inversion by such PE is driven by repulsive correlations of PE turns at the macroion surface. Such correlations make an almost equidistant solenoid (see Fig. 1), which locally resembles one-dimensional Wigner crystal along the direction perpendicular to PE. In the absence of salt, the charge inversion ratio is smaller than 100%. In a salty solution, it grows with the salt concentration. When the Debye-Hückel screening radius r_s becomes smaller

than the distance between neighboring turns A, the charge inversion ratio can be larger than 100%.

The charge inversion of a macroion due to complexation with one PE molecule can be explained in the way similar to Refs. [7,8], which dealt with the charge inversion of a macroion screened by many rigid multivalent counterions (Z-ions). The tail repels adsorbed PE and creates correlation hole or, in other words, its positively charged image. This image in the already adsorbed layer of PE is responsible for the additional correlation attraction to the surface, which leads to the charge inversion.

We show that smearing of charge PE on the surface of the sphere employed in Ref. [3] is a good approximation only at $A \sim a$. If $A \gg a$ smearing of charge at the surface of sphere is a rough approximation and leads to anomalously strong inversion of charge and to the unphysical independence of the inverted charge Q^* on Q. The reason of this phenomenon is easy to understand. Smearing means that the PE solenoid is assumed to behave as a perfect metal. A neutral metal surface can adsorb a charged PE due to image forces, making the charge inversion ratio infinite. In reality, for an insulating macroion, an image of a point charge in the PE coil can not be smaller than A and the energy of attraction to it vanishes at growing A. Only a macroion with a finite charge Q adsorbs a PE coil with a finite A. Therefore, Q^* depends on Q and the charge inversion ratio is always finite.

Our analytic theory is followed by Monte-Carlo simulations. They demonstrate good agreement with the theory.

II. AN ANALYTICAL THEORY.

For a quantitative calculation, consider the complexation of a negative PE with linear charge density $-\eta$ and length L, with a spherical macroion with radius R and positive charge Q. We assume that the PE is weakly charged, i. e. $\eta \ll \eta_c$, where $\eta_c = k_B T D/e$ is Onsager-Manning critical linear density, T is the temperature, k_B is the Boltzmann constant and D is the dielectric constant of water. In this case, there is no Onsager-Manning condensation

of counterions and one can use linear theory of screening. Because we are interested in the charge inversion of the complex, we assume that the PE length L is greater than the neutralizing length $\mathcal{L} = Q/\eta$. In this case, a finite length L_1 of the PE is tightly wound around the macroion due to the electrostatic attraction. The rest of the PE with length $L_2 = L - L_1$ can be arranged into two possible configurations: one tail with length L_2 or two tails with length $L_2/2$ going in opposite directions radially outwards from the center of the macroion. In both cases, the tails are straight to minimize its electrostatic self-energy. We assume that $\mathcal{L} \gg R$, so that there are many turns of the PE around the sphere. Our goal is to calculate the net charge of the complex $Q^* = Q - L_1\eta = (\mathcal{L} - L_1)\eta$ and the charge inversion ratio $|Q^*|/Q$. We show that, in the most common configuration with one tail, this net charge is negative: more PE winds around the macroion than it is necessary to neutralize it.

Let us start from the salt free solution in which all Coulomb interactions are not screened. For simplicity, we assume that the PE has no intrinsic rigidity, but its linear charge density is large so that it has a rod-like configuration in solution due to Coulomb repulsion between monomers. When PE winds around the macroion, the strong Coulomb repulsion between the neighboring PE turns keeps them parallel to each other and establishes an almost constant distance A between them (Fig. 1). The total energy of the macroion with the PE solenoid wound around it, F_1, can be written as a sum of the Coulomb energy of its net charge plus the self-energy of PE:

$$F_1 = (L_1 - \mathcal{L})^2/2R + L_1 \ln(A/a) . \tag{1}$$

Here and below we write all energies in units of η^2/D, where D is dielectric constant of water (thus, all energies have the dimensionality of length.) The second term in Eq. (1) deserves special attention. The self-energy of a straight PE of length L_1 in the solution is $L_1 \ln(L_1/a)$. However, when it winds around the macroion, every turn is effectively screened by the neighboring turns at the distance A. This screening brings the self-energy down to $L_1 \ln(A/a)$. At length scale greater than A, the surface charge density of the spherical

complex is uniform and the excess charge $L_1 - \mathcal{L}$ is taken into account by the first term in Eq. (1). In other words, one can interpret Eq. (1) thinking about our system as the superposition of a uniformly charged sphere with charge $(L_1 - \mathcal{L})$ and a neutral complex consisting of the solenoid on a neutralizing spherical background. The total energy of these two objects is additive. Indeed, the energy of interaction between them vanishes because the first one creates a constant potential on the second neutral one.

One can also rewrite the energy of solenoid on the neutralizing background as

$$L_1 \ln(A/a) = L_1 \ln(R/a) - L_1 \ln(R/A) . \tag{2}$$

Here the first term is the self-energy of the PE with length L_1 whose turns are randomly positioned on the macroion. (Indeed, for a strongly charged PE, each PE turn is straight up to a distance of the order of R due to its electrostatic rigidity. If we keep a PE turn fixed and average over random positions of all other turns we find our turn on the uniform spherical background of opposite charge. The absolute value of the background charge is of the order R, the energy of interaction of our turn with it is of the order R and is negligible compared to the turn's self-energy $R \ln(R/a)$ or $\ln(R/a)$ per unit length.) Now it is easy to identify the second term of Eq. (2) as the correlation energy. It represents the lowering of the system's energy by forming an equidistant coil from the random one. This correlation energy, E_{cor}, is of the order of the interaction of the PE turn with its background (a stripe of of the length R and the width A of the surface charge of the macroion) because all other turns lie at the distance A and beyond. Estimating $A \sim R^2/L_1$, we can write

$$E_{cor} \simeq -L_1 \ln(R/A) \simeq -L_1 \ln(L_1/R). \tag{3}$$

Substituting Eqs. (3) and (2) into Eq. (1) for the total energy of the spherical complex, we obtain

$$F_1 = L_1 \ln(R/a) - L_1 \ln(L_1/R) + (L_1 - \mathcal{L})^2/2R . \tag{4}$$

To take into account the PE tails, let us consider each tail configuration separately.

One tail configuration. In this case, the total free energy of the system is the sum of that of the spherical complex, the self-energy of the tail and their interaction. This gives:

$$F = F_1 + L_2 \ln(L_2/a) + (L_1 - \mathcal{L}) \ln\left[(L_2 + R)/R\right] \ . \tag{5}$$

To find the optimum value of the length L_1 one has to minimize F with respect to L_1. Using Eq. (5) and the relation $L_2 = L - L_1$, we obtain

$$(L_1 - \mathcal{L})\left[R^{-1} - (L - L_1 + R)^{-1}\right] = \ln(\mathcal{L}/R) \ , \tag{6}$$

where we neglected terms of the order of unity and took into account that $L_2 \gg R$ (as shown below, Eq. (8)). The physical meaning of Eq. (6) is transparent: The left side is the energy of the Coulomb repulsion of the net charge of the spherical complex which has to be overcome in order to bring an unit length of the PE from the tail to the sphere. The right hand side (in which, L_1 has been approximated by $\mathcal{L}$) is the absolute value of the correlation energy gained at the sphere which helps to overcome this repulsion (See Eq. (3)). Equilibrium is reached when these two forces are equal. From Eq. (6), one can easily see that $L_1 - \mathcal{L}$ is positive, indicating a charge inversion scenario: more PE collapses on the macroion than it is necessary to neutralize it. Eq. (6) also clearly shows that correlations are the driving force of charge inversion.

To understand how the length L_1 varies for different PE length L, it is instructive to solve Eq. (6) graphically. One can see the following behavior (Fig. 2):

(a) When $L - \mathcal{L}$ is small, Eq. (6) has no solutions, $\partial F/\partial L_1$ is always negative. The free energy is a monotonically decreasing function of L_1 and is minimal when $L_1 = L$. In this regime, the whole PE collapses on the macroion.

(b) As L increases beyond a length L^*, Eq. (6) acquires two solutions, which correspond to a local minimum and a local maximum in the free energy as a function of L_1. The global minimum is still at $L_1 = L$ and the whole PE remains in the collapsed state.

(c) When L increases further, at a length $L = L_c$, the local minimum in the free energy at $L_1 < L$ becomes smaller than the minimum at $L_1 = L$. A first order phase transition

6

happens and a tail with a finite length L_2 appears. L_c can be found from the requirement that the equation $F(L_1) - F(L) = 0$ has solutions at $0 < L_1 < L$. Using Eq. (5), one gets

$$L_c \simeq \mathcal{L} + R\ln(\mathcal{L}/R) + R\sqrt{\ln(\mathcal{L}/R)}\sqrt{\ln\ln(\mathcal{L}/R)}, \tag{7}$$

and the tail length L_2 at this critical point is

$$L_{2,c} \simeq R\sqrt{\ln(\mathcal{L}/R)}\sqrt{\ln\ln(\mathcal{L}/R)} . \tag{8}$$

As L continues to increase, L_1 decreases and eventually saturates at the constant value

$$L_{1,\infty} = \mathcal{L} + R\ln(\mathcal{L}/R) \simeq L_c - L_{2,c} , \tag{9}$$

which can be found from Eq. (6) by letting $L \to \infty$. Eq. (7) - (9) are asymptotic results valid at $\mathcal{L}//R \to \infty$. If $\mathcal{L}//R$ is not very large one can find $L_1(L)$ minimizing Eq. (5) numerically. In Fig. 3 we present results for the case $\mathcal{L} = 25R$, which corresponds to $25/2\pi \simeq 4$ turns. In this case, $L_c = 35.5R$, $L_{2,c} = 4.0R$ and $L_{1,\infty} = 30.4R$. It should be also noted that, as Fig. 3 and Eqs. (7), (8) and (9) suggest, L_1 is almost equal $L_{1,\infty}$ after the phase transition.

At $\mathcal{L} \gg R$, the charge inversion ratio $|Q^*|/Q = (L_1 - \mathcal{L})/\mathcal{L}$ can be calculated from Eqs. (7) and (9): $|Q^*|/Q = (R/\mathcal{L})\ln(\mathcal{L}/R) \ll 1$. Thus, the charge inversion ratio is only logarithmically larger than the inverse number of PE turns in the coil.

Using the insight gained above, we are now in a position to achieve better understanding of the nature of the approximation employed in Ref. [3]. The authors of Ref. [3] replaced the adsorbed PE by the same charge uniformly smeared at the macroion surface. Therefore, the term $L_1\ln(A/a)$ was omitted in Eq. (1), so that at $A \gg a$, the correlation energy was overestimated. This approximation replaces the right hand side of Eq. (6) by the self-energy of a unit length of the tail. Correspondingly, Eq. (6) now balances the self-energy of a unit length of the tail with the electrostatic energy of this unit length smeared at the surface of overcharged macroion. Thus we can call this mechanism of charge inversion "the elimination of the self-energy" or simply "metallization".

As a result, the charge inversion obtained in Ref. [3], at $A \gg a$, is larger than that of our paper. (Our correlation mechanism can be interpreted as a partial elimination of the self-energy. The second term of Eq. (1) is what is left from the PE self-energy due to self screening of PE at the distance A.) Surprising independence of Q^* on Q or, in other words, the possibility of an infinite charge inversion ratio obtained in Ref. [3] is also related to smearing of PE on the macroion surface. This happens because when PE arrives at the macroion surface it looses all its (positive) self-energy. This brings about an energy gain which does not depend on the bare charge of the macroion.

On the other hand, at $A \sim a$, the smearing of PE is a good approximation and our results are close to that of Ref. [3].

Two tails configuration. The free energy of the system can be written similar to Eq. (5), keeping in mind that we have two tails instead of one, each with length $L_2/2$:

$$F = F_1 + L_2 \ln \frac{L_2}{2a} + 2(L_1 - \mathcal{L}) \ln \frac{L_2 + 2R}{2R} +$$
$$+(L_2 + 2R) \ln \frac{L_2 + 2R}{2R} - (L_2 + 4R) \ln \frac{L_2 + 4R}{4R}. \tag{10}$$

The last two terms describe the interaction between the tails. The optimum length L_1 can be found from the condition of a minimum in the free energy. Taking into account that, as shown below, $L_2 \gg R$ and ignoring terms of the order unity, one gets

$$(L_1 - \mathcal{L}) \left[R^{-1} - (L_2/2 + R)^{-1} \right] + \ln(L_2/R) = \ln(\mathcal{L}/R) . \tag{11}$$

Comparing this equation to Eq. (6), one finds an additional potential energy cost $\ln(L_2/R)$ for bringing a unit length of the PE from the end of a tail to the sphere. It originates from the interaction of this segment with the other tail. When L is not very large, $L_2 \ll \mathcal{L}$, one can neglect this additional term and the two tail system behaves like the one tail one. At a small L, the whole PE lies on the macroion surface and the system is overcharged. As L increases, eventually a first order phase transition happens, where two tails with length of the order $R\sqrt{\ln(\mathcal{L}/R)}$ appear. On the other hand, when L is very large, such that $L_2 \gg \mathcal{L}$, the new term dominates and the macroion becomes undercharged ($L_1 - \mathcal{L}$ is negative) with

8

L_1 decreasing as a logarithmic function of the PE length: $L_1 \simeq \mathcal{L} - R\ln(L/\mathcal{L})$. At an exponentially large value of $L \sim \mathcal{L}\exp(\mathcal{L}/R)$, the length L_1 reaches zero and the whole PE unwinds from the macroion.

Above, we have described configurations with one tail and two tails separately. One should ask which of them is realized at a given L. Numerical calculations show that, when L is not very large, the overcharged, one tail configuration is lower in energy. At a very large value of L, the complex undergoes a first order phase transition to a two tails configuration and becomes undercharged. The value of this critical length L_{cc} can be estimated by equating the free energies (5) and (10) at their optimal values of L_1 which are $\mathcal{L} + R\ln(\mathcal{L}/R)$ and $\mathcal{L} - R\ln(L/\mathcal{L})$ respectively. In the limit where $\ln(\mathcal{L}/R) \gg 1$, keeping only highest order terms, we get $L_{cc} \sim \mathcal{L}^2/R$, which indeed is a very large length scale. This order of appearance of one and two tail configurations is in disagreement with Ref. [3].

In practical situations, there is always a finite salt concentration in a water solution. One, therefore, has to take the finite screening length r_s into account. For any reasonable r_s, $L_{cc} \gg r_s$, and all Coulomb interactions responsible for the transition from one to two tails are screened out. Therefore, in a salty solution the two tail configuration disappears. Below we concentrate on the effect of screening on one tail or tail-less configurations only.

In a weak screening case, when $r_s \gg L_{2,c}$, Coulomb interactions responsible for the appearance of the tail remain unscreened. Therefore, the lengths L_c and $L_{2,c}$ remain almost unchanged. The large L limit of L_1 however should be modified. At a very large tail length L_2 one should replace $L - L_1 = L_2$ by r_s in Eq. (6) because the potential vanishes beyond the distance r_s. This gives

$$L_{1,\infty}(r_s) = \mathcal{L} + R\ln(\mathcal{L}/R) + (R^2/r_s)\ln(\mathcal{L}/R) \quad .$$

One can see that $L_{1,\infty}$ increases and charge inversion is stronger as r_s decreases. This is because when r_s decreases, the capacitance of the spherical complex increases, the self-energy of it decreases and it is easier to charge it.

When $R < r_s < L_{2,c}$, it is easy to show that the tail length, which appears at the phase

transition, is equal to r_s instead of $L_{2,c}$. This means that, before a tail is driven out at the phase transition, more PE condenses on the macroion in a salty solution than that for the salt free case. In other words, the critical point L_c is shifted towards larger values:

$$L_c(r_s) = L_{1,\infty}(r_s) + r_s \quad .$$

Obviously, $L_c(r_s) > L_c$ for $r_s < L_{2,c}$ and $L_c(r_s)$ approaches L_c at $r_s \sim L_{2,c}$. When r_s approaches R, the critical length $L_c(r_s)$ reaches $\mathcal{L} + 2R\ln(\mathcal{L}/R)$, so that the inverted charge is twice as large as that for the unscreened case.

At stronger screening, when $r_s < R$, to a first approximation, the macroion surface can be considered as a charged plane. The problem of adsorption of many rigid PE molecules on an oppositely charged plane has been studied in Ref. [8], where the role of Wigner crystal like correlations similar to that shown in Fig. 1 was emphasized. The large electrostatic rigidity of a strongly charged PE makes this calculation applicable to our problem as well. One can use results of Ref. [8] in three different ranges of r_s: $R > r_s > A$, $A > r_s > a$, $a > r_s$. In all these ranges, the net charge Q^* of the macroion is proportional to R^2 instead of an almost linear dependence on R in a salt free solution. The tail is not important for the calculation of the charge inversion ratio because it produces only a local effect near the place where the tail stems from the macroion. Inverted net charge Q^* grows with decreasing r_s, so that charge inversion ratio of the macroion reaches 100% at $r_s \sim A$ and can become even larger at $r_s \ll A$. For $r_s \ll A$, our results are in agreement with those of Ref. [5,9]. One should be aware that $|Q^*|$ ceases to increase at very small r_s. This is because at an extremely small r_s such that the interaction between the macroion and one persistence length of the PE becomes less than k_BT, the PE desorbs from the macroion and the macroion becomes undercharged. Therefore, $|Q^*|$ should reach a maximum at a very small r_s and then decrease.

Finally, it should be noted that in the above discussion of the role of screening, we neglected the possibility of the condensation of the PE's counterions on the sphere with inverted charge. This is valid for a large enough screening length because it is well known that in this case condensation does not occurs on a spherical macroion. Using $Q^* \sim R\ln(\mathcal{L}/R)$

10

and the standard condition for the condensation on a charged sphere [10], it is not difficult to show that the sphere is screened linearly if

$$r_s > R^{1-\eta/2\eta_c} \mathcal{L}^{\eta/2\eta_c} \quad .$$

When $r_s < R$, the macroion can be approximated as a charged plane and it is also known that a planar charge is linearly screened if the screening radius is small enough. Specifically, Eq. (73) of Ref. [8] shows that screening is linear if

$$r_s < A e^{\eta_c/\eta} \sim \frac{R^2}{\mathcal{L}} e^{\eta_c/\eta} \quad .$$

As we can see, when η is less than η_c by a logarithmic factor, i. e. when $\eta < \eta_c/\ln(\mathcal{L}/R)$, the range of r_s, where the macroion is nonlinear screened, almost vanishes. For η of the order of η_c, however, there is a range of r_s where counterion condensation on the charge-inverted sphere has to be taken into account and the sphere's net charge is different from our estimate. There are two aspects of this counterion condensation phenomenon. Obviously, due to stronger nonlinear screening at the sphere surface, more PE collapses onto the sphere and the charge inversion ratio is even larger than what is predicted above in the linear screening theory. On the other hand, if one defines the net charge of the sphere as the sum of its bare charge, the charges of the collapsed PE monomers and the charges of all counterions condensed on it, the magnitude of this net charge is limited at the value given by the theory of counterion condensation on a sphere [10]. As explained in Ref. [8], it is this charge that is observed in electrophoresis.

Until now we talked about a weakly charged PE with $\eta \leq \eta_c$. In Ref. [8] we studied adsorption of a strongly charged PE (for e.g., DNA) with $\eta \gg \eta_c$ on positively charged plane. Such PE initiates Onsager-Manning counterion condensation both in the bulk and at the plane. The theory Ref. [8] can be applied for the sphere at $r_s \ll R$, too. It predicts a strong charge inversion which grows with decreasing r_s and exceeds 100% at $r_s < A$.

III. MONTE-CARLO SIMULATIONS.

To verify the results of our analytical theory, we do Monte Carlo (MC) simulations. The PE is modeled as a chain of N freely jointed hard spherical beads each with charge $-e$ and radius $a = 0.2l_B$ where $l_B = 7.12\text{Å}$ is the Bjerrum length at room temperature $T_{rm} = 298°\text{K}$ in water. The bond length is kept fixed and equal to l_B, so that our PE charge density η is equal to the Manning condensation critical charge density $\eta_c = k_B T_{rm} D/e$. Due to the discrete nature of the simulated PE, in order to compare simulation results with theoretical predictions, we refer to the number of monomers N as the PE length L measured in units of l_B. The macroion is modeled as a sphere of radius $4l_B$ and with charge $100e$ uniformly distributed at its surface. To arrange the configuration of the PE globally, the pivot algorithm is used. In this algorithm, a part of the chain from a randomly chosen monomer to one of the chain ends is rotated by a random angle about a random axis (see Ref. [1] and references therein). To relax the PE configuration locally, a flip algorithm is used. In this algorithm, a randomly selected monomer is rotated by a random angle about the axis connecting its two neighbors (if it is one of the end monomers, its new position is chosen randomly at a sphere of radius l_B centered at its neighbor). The usual Metropolis algorithm is used to accept or reject the move. For a typical value of the parameters, we run about 10^7 Monte Carlo steps and used the last 70% of them to obtain statistical averages (one Monte Carlo step is defined as the number of elementary moves such that, on average, every particle attempts to move once). Near the phase transition to the tail state, the number of steps is 5 times larger. The time for one run is typically 5 hours on an Athlon 1 Ghz computer. Assembler language is used to speed up the calculation time inside the inner loop of the program. Our code was checked by comparing with the results of Ref. [1] and Ref. [3] and some references therein.

Two different initial conformations of the PE are used to make sure that the system is in equilibrium. In the first initial conformation, the PE forms an equidistant coil around the macroion. In the second initial conformation, the PE makes a straight rod. Both initial

conformations, within statistical uncertainty, give the same values for all the calculated properties of the systems such as the total energy, the end-end distance of the PE, the number of collapsed monomers and the critical length L_c.

An important aspect of the simulation is to determine the length of the tail and the amount of monomers residing at the macroion surface. In the literature, one usually defines a monomer as collapsed on the surface if it is found within a certain distance from it. This distance is arbitrarily chosen to be about two or three PE bond lengths. In the Appendix, we suggest an alternative more systematic method of determining the number of collapsed monomers.

Let us now describe the results of our Monte-Carlo simulations. We study the collapsed length L_1 as a function of L for the case the macroion has radius $R = 4l_B$ and charge $Q = 100e$. This corresponds to $\mathcal{L}/R = 25$, exactly the same value as the one used in Fig. 3. The result of our simulation is presented in Fig. 4 together with the theoretical curve of Fig. 3. The phase transition is observed at the chain length of 142 monomers and the critical tail length is about 16 monomers, which agrees very well with our predictions $L_c = 142$ and $L_{2c} = 16$.

We also study the case of a salty in solution. As everywhere in this paper, we assume that screening by monovalent salt can be described in the linear Debye-Hückel approximation. Therefore, in our simulation, we replace the Coulomb potential of the macroion Q/Dr by the screened potential

$$V(r) = \frac{Qe^{R/r_s}}{1 + R/r_s} \frac{e^{-r/r_s}}{Dr} \quad , \tag{12}$$

where r_s is the linear Debye-Hückel screening length. All PE monomers are still considered as point-like charges and Yukawa potential, $r^{-1}e^{-r/r_s}$, is used to describe their interaction. The result of our simulation for the case $r_s = 5l_B$ is plotted by the solid square in Fig. 4. As predicted above, screening increases the maximum charge inversion ratio to 63%.

Simulation at $r_s = 4l_B$ shows even bigger charge inversion with 70% ratio. This suggests that the maximum in charge inversion is located at even smaller screening radius. How-

ever, we did not try to run the simulation at smaller r_s in order to find the maximum in charge inversion because, at smaller r_s, the identification of adsorbed monomers becomes less unambiguous.

The better-than-expected agreement between MC results and theoretical prediction of the critical length L_c for the $r_s = \infty$ case is somewhat accidental because in Fig. 4 we compared a zero temperature theory with a finite temperature Monte-Carlo simulation. The temperature affects L_c because tail monomers have smaller entropy compared to collapsed monomers. The self repulsion of the tail and the repulsion from the overcharged sphere limits the configuration space of the tail monomers, while at the macroion, the PE self-energy is screened at the distance A, so that the collapsed monomers have larger configuration space. Therefore, the free energy is gained when more monomers collapse on the macroion surface. This helps to push the critical length L_c to a higher value than its value at zero temperature.

For clarifying the role of temperature, we carry out simulations at different T and extrapolate L_c to $T = 0°$K. The results are shown in Fig. 5. The extrapolated L_c is 134 which is 6% lower than the zero temperature theoretical prediction of 142. Also from this figure, one can see that the temperature dependence of L_c is linear. A simple analysis of the Monte-Carlo data shows that the entropy per monomers gained at the surface is about 2 at the critical point.

On Fig. 6 we show two typical snapshots of the system, one for the case $L = 141$ (before the phase transition) and the other for $L = 143$ (after the phase transition). They again confirm that the tail appears abruptly near $L = L_c = 142$. One can clearly see an important aspect of the correlation effects: PE segments of different turns stay away from each other and locally, they resemble a one dimensional Wigner crystal, which helps to lower the energy of the system. Globally, however, the PE conformation resembles that of a tennis ball instead of a solenoid. This obvious difference between observed conformation and the theoretical solenoid-like ground state is also related to thermal fluctuations. Solenoid structure is subjected to low energy long range bending modes, energy of which is proportional to k^4, where k is the wave vector of such mode. It is easy to show that at the room tem-

perature with our parameters of the system, modes with $k \sim R^{-1}$ are strongly excited and they "melt" the solenoid. However, modes with large k are not excited and, therefore, the short range order between PE turns is preserved. This leads to a compromised "tennis ball" conformation instead of a solenoid. The difference in energy between a "tennis ball" and a solenoid conformation, however, is small compare to the interaction between the sphere and the PE. This helps to explain the small difference between the results of the finite temperature Monte-Carlo simulation and our zero temperature theory.

Monte-Carlo results similar to Fig. 4 for unscreened case were independently obtained in Ref. [11]. For the screened case, however, the authors of Ref. [11] claimed that charge inversion reaches maximum when $r_s \simeq 3R$ which is still very large, much larger than what is observed in our simulations. This is because instead of the Overbeck potential (12), the authors of Ref. [11] use the Yukawa potential $Qr^{-1}e^{-r/r_s}$ for the macroion, where r is the distance to the center of the macroion. This means that they put the net charge of the macroion at the center and screen it inside the macroion body. As a result, the apparent surface charge of the macroion becomes very small and charge inversion disappears. New simulations [12] carried out by the same authors using the proper potential (12) are in agreement with our theory and Monte Carlo simulations.

Before concluding this paper, we would like to mention that in our simulation, counterion condensation on the sphere with inverted charge was neglected. As stated in the end of Sec. II, this is valid if $\eta \ll \eta_c$. In our Monte-Carlo simulations η is equal to η_c therefore, in order to study the effect of screening on charge inversion, we choose to simulate the system at small $r_s \sim A$ where condensation is not very important.

In conclusion, we have studied charge inversion for the complexation of a PE with a spherical macroion. We started from description of the correlated ground state configuration of PE at the macroion surface instead of smearing of the PE charge at the surface. As a result, we have eliminated the unphysical finite charge adsorption at the neutral sphere. Our Monte-Carlo simulations confirm that correlations are the driving force of charge inversion.

APPENDIX A: THE NUMBER OF COLLAPSED MONOMERS OF POLYELECTROLYTE.

To better determine the number of collapsed monomers in Monte-Carlo simulation, we use the following procedure.

Firstly, we draw the histogram of the number of monomers found within a distance r from the macroion surface during a simulation run. Up to a normalizing factor, this histogram is nothing but the probability $P_r(n)$ of finding n monomers within a distance r from the sphere surface. Secondly, at a given r, we define the value of n corresponding to the maximum in this histogram as the most likely number of monomers $n(r)$ found inside the distance r from the macroion surface.

Now, we show that much can be learned by plotting $n(r)$ as a function of r. In Fig. 7a, $n(r)$ is plotted for two typical cases of $L = 140$ (before the phase transition) and $L = 150$ (after the phase transition).

Clearly, as one goes away from the macroion surface, or r grows, at first one see a rapid increase in the number of monomers $n(r)$ found. After a distance of about two bond lengths, this increase is slowed and stopped. It is easy to identify the first range of r, where one observes a rapid increase in $n(r)$ as the collapsed layer. For the case of $L = 140$, as r increases beyond this layer, $n(r)$ is always equal to the total number of monomers $N = 140$. This is the indication of a collapsed state where all PE monomers lie in the collapsed layer near the macroion surface. The situation is completely different in the case of $L = 150$ where beyond the collapsed layer one sees a linear increase in $n(r)$ until $r = 19$ (not shown)

16

where $n(r)$ saturates at the maximum possible value of 150. This is an indication of a tailed state. The slope of the increase in this second range also provides a valuable information on the conformation of the tailed state. As one can see, this slope is very close to unity, what clearly indicates a one-tail state. This is in agreement with our prediction that after the phase transition the complex is in one tail state and in disagreement with the conclusion of Ref. [3] that the system fluctuates between one tail and two tail conformations (for a two tail state the slope would be 2).

A closer look at the tail part of Fig. 7 shows that the slope of the tail part of $n(r)$ actually is slightly larger than unity and grows with r. This could be expected. The PE tail near the overcharged macroion is strongly stressed in the electric field of the macroion's inverted charge. Farther from the macroion, this electric field is weaker and due to the thermal motion of the monomers, more than one monomer can be found as r increases by one bond length.

The final step in determining the number of collapsed monomers in the tailed state is accomplished by fitting the tail part of $n(r)$ by an empirical quadratic equation $ax^2 + bx + c$. The intersection of this curve with the y axis gives the number of collapsed monomers or the collapsed length L_1. For e.g., at $L = 150$, the value of a, b and c are 0.01, 1.22 and 125 respectively (see Fig. 7b), so that the slope at the macroion surface $x = 0$ is 1.22 and the amount of collapsed monomers is 125. Also, as L increase, the tail gets longer and becomes more stressed due to its self-energy, the slope of $n(r)$ decreases and is closer to 1. The fitted value for b are 1.32 at $L = 145$, 1.22 at $L = 150$ and 1.09 at $L = 165$.

Near the phase transition point $L = 142$ one sees two maxima in the histogram $P_r(n)$ instead of one. One of these maxima behaves exactly as that of one tail configuration (linearly increases with r after the collapsed layer). The other maximum behaves exactly as that of the collapsed state (constant and equal the total number of monomers $N = 142$ after the collapsed layer). This is because near the phase transition the PE fluctuates between the collapsed and the tailed state.

REFERENCES

[1] Wallin T. and Linse P., Langmuir **12**, (1996) 305.

[2] Wang Y., Kimura K., Huang Q., Dubin P. L. and Jaeger W., Macromolecules **32** (1999) 7128.

[3] Mateescu E. M., Jeppersen C. and Pincus P., Europhys. Lett. **46** (1999) 454.

[4] Park S. Y., Bruinsma R. F. and Gelbart W. M., Europhys. Lett. **46** (1999) 493.

[5] Netz R. R. and Joanny J. F., Macromolecules, **32** (1999) 9026.

[6] Sens P. and Gurovitch E., Phys. Rev. Lett., **82** (1999) 339.

[7] Perel V. I. and Shklovskii B. I., Physica A, **274**(1999) 446; Shklovskii B. I., Phys. Rev. E, **60** (1999) 5802.

[8] Nguyen T. T., Grosberg A. Yu. and Shklovskii B. I., J. Chem. Phys.,**113**(2000) 1110.

[9] A. V. Dobrynin, A. Deshkovski and M. Rubinstein, Macromolecules 2000.

[10] M. Guerom, G. Weisbuch, Biopolimers, **19**, 353 (1980); S. Alexander, P. M. Chaikin, P. Grant, G. J. Morales, P. Pincus, and D. Hone, J. Chem. Phys. **80**, 5776 (1984); S. A. Safran, P. A. Pincus, M. E. Cates, F. C. MacKintosh, J. Phys. (France) **51**, 503 (1990); L. Belloni, Doctoral thesis, University of Paris IV (1982); Chem. Phys. **99** 43 (1985).

[11] Chodanowski P. and Stoll S., Macromolecules 2000.

[12] Chodanowski P., PhD thesis, University of Geneva, 2001.

FIGURES

FIG. 1. The PE winds around a spherical macroion. Due to their Coulomb repulsion, neighboring turns lie parallel to each other. Locally, they resemble a one-dimensional Wigner crystal with the lattice constant A.

FIG. 2. Schematic plots of the free energy as function of the collapsed length L_1 at different values of L: a) $\mathcal{L} < L < L^*$, b) $L^* < L < L_c$, c) $L > L_c$.

FIG. 3. The collapsed length L_1 (solid line) and the tail length L_2 (dashed line) *vs.* the total PE length L. A first order phase transition happens at $L = L_c$ where a tail with a finite length $L_{2,c}$ appears.

FIG. 4. The first order phase transition to the tailed state with increasing L at $\mathcal{L}/R = 25$. The solid line is the theoretical prediction of the collapsed length L_1 as function of the PE length L (same as the one plotted in Fig. 3). The solid circles are MC results at $r_s = \infty$. The solid squares are MC results at $r_s = 5l_B$. The dotted line is a guide to the eyes.

FIG. 5. The critical length L_c as a function of temperature. Because the entropy is proportional to the number of collapsed monomers, a linear fit (the dashed line) is used to extrapolate to zero temperature. The line has equation $y = 0.029 * x + 133.61$. Thus $L_c \simeq 134$ at $T = 0 °$K.

FIG. 6. Two snapshot of the system for the cases $L = 141$ (right sphere) and $L = 143$ (left sphere).

FIG. 7. The most likely number of monomers $n(r)$ found within a distance r (measured in units of l_B) from the macroion surface. a) two typical plots of $n(r)$: one for the case $L = 140$ (below the transition length $L_c = 143$) and the other for the case $L = 150$ (above L_c). b) quadratic fit for the tail part of $n(r)$ for $L = 150$. The dotted line is the fitted function $f(x) = 0.0098x^2 + 1.22x + 125$.
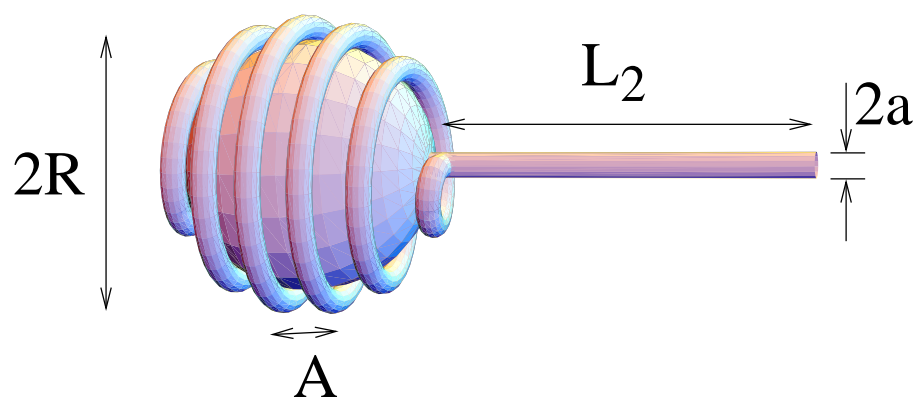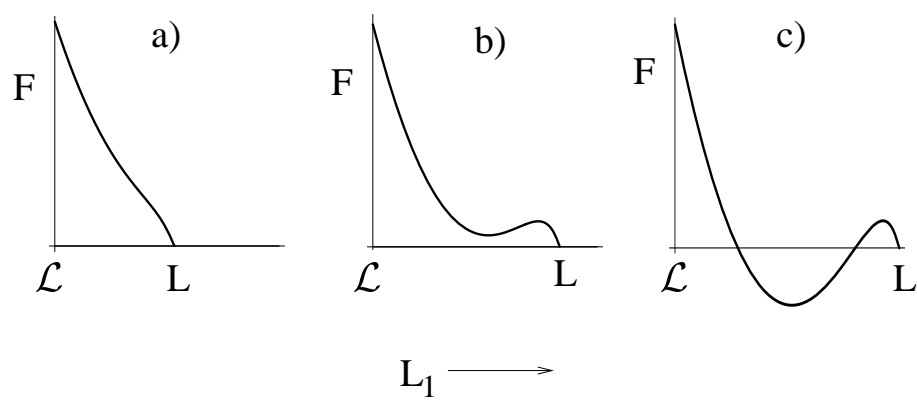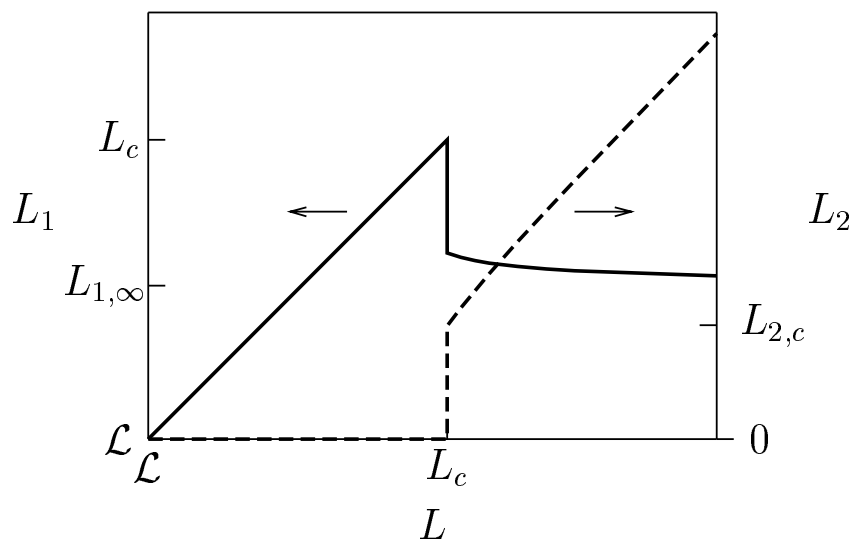
FIGURE 1
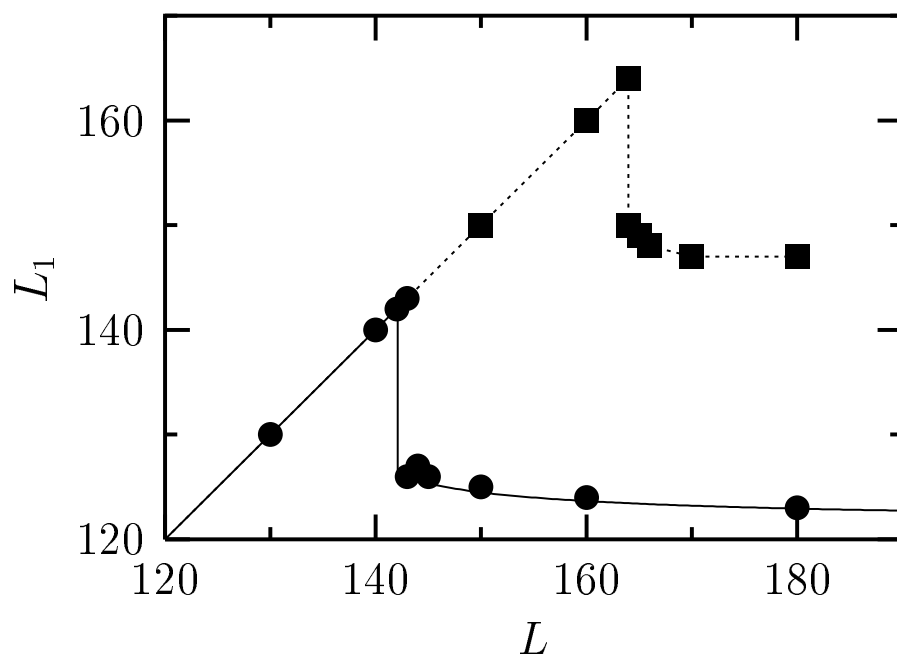
FIGURE 2

FIGURE 3

FIGURE 4

FIGURE 5

FIGURE 6

$$L = 141$$

$$L = 143$$

FIGURE 7